ESC HEART FAILURE
ESC Heart Failure 2022; **9**: 1976–1986
Published online 25 March 2022 in Wiley Online Library (wileyonlinelibrary.com) **DOI:** 10.1002/ehf2.13909

ORIGINAL ARTICLE

Utility of left atrial and ventricular strain for diagnosis of transthyretin amyloid cardiomyopathy in aortic stenosis

Fumi Oike[1,2], Hiroki Usuku[1,2,3], Eiichiro Yamamoto[1,2]*, Kyohei Marume[1,2], Seiji Takashio[1,2], Masanobu Ishii[1,2], Noriaki Tabata[1,2], Koichiro Fujisue[1,2], Kenshi Yamanaga[1,2], Daisuke Sueta[1,2], Shinsuke Hanatani[1,2], Yuichiro Arima[1,2], Satoshi Araki[1,2], Seitaro Oda[4], Hiroaki Kawano[1,2], Hirofumi Soejima[1,2], Kenichi Matsushita[1,2], Mitsuharu Ueda[5], Toshihiro Fukui[6] and Kenichi Tsujita[1,2]

[1]*Department of Cardiovascular Medicine, Faculty of Life Sciences, Graduate School of Medical Sciences, Kumamoto University, 1-1-1 Honjo, Chuo-ku, Kumamoto, 860-8556, Japan;* [2]*Center of Metabolic Regulation of Healthy Aging, Faculty of Life Sciences, Kumamoto University, Kumamoto, Japan;* [3]*Department of Laboratory Medicine, Kumamoto University Hospital, Kumamoto, Japan;* [4]*Department of Diagnostic Radiology, Faculty of Life Sciences, Kumamoto University, Kumamoto, Japan;* [5]*Department of Neurology, Graduate School of Medical Sciences, Kumamoto University, Kumamoto, Japan; and* [6]*Department of Cardiovascular Surgery, Graduate School of Medical Sciences, Kumamoto University, Kumamoto, Japan*

Abstract

Aims To clarify the usefulness of left atrial (LA) function and left ventricular (LV) function obtained by two-dimensional (2D) speckle tracking echocardiography to diagnose concomitant transthyretin amyloid cardiomyopathy (ATTR-CM) in patients with aortic stenosis (AS).

Methods and results We analysed 72 consecutive patients with moderate to severe AS who underwent ^{99m}Tc-pyrophosphate (PYP) scintigraphy at Kumamoto University Hospital from January 2012 to September 2020. We divided these 72 patients into 2 groups based on their ^{99m}Tc-PYP scintigraphy positivity or negativity. Among 72 patients, 16 patients (22%) were positive, and 56 patients (78%) were negative for ^{99m}Tc-PYP scintigraphy. In clinical baseline characteristics, natural logarithm troponin T was significantly higher in the ^{99m}Tc-PYP scintigraphy-positive than scintigraphy-negative group (-2.9 ± 0.5 vs. -3.5 ± 0.8 ng/mL, $P < 0.05$). In conventional echocardiography, the severity of AS was not significantly different between these two groups. In 2D speckle tracking echocardiography, the relative apical longitudinal strain (LS) index (RapLSI) [apical LS/ (basal LS + mid LS)] was significantly higher (1.09 ± 0.49 vs. 0.78 ± 0.23, $P < 0.05$) and the peak longitudinal strain rate (LSR) in LA was significantly lower in the ^{99m}Tc-PYP scintigraphy-positive than scintigraphy-negative group (0.36 ± 0.14 vs. 0.55 ± 0.20 s^{-1}, $P < 0.05$). Multivariable logistic analysis revealed the peak LSR in LA and RapLSI were significantly associated with ^{99m}Tc-PYP scintigraphy positivity. Receiver operating characteristic analysis showed that the area under the curve (AUC) of the peak LSR in LA for ^{99m}Tc-PYP scintigraphy positivity was 0.79 and that the best cut-off value of the peak LSR in LA was 0.47 s^{-1} (sensitivity: 78.6% and specificity: 72.3%). The AUC of RapLSI for ^{99m}Tc-PYP scintigraphy positivity was 0.69, and the cut-off value of RapLSI was decided as 1.00 (sensitivity: 43.8% and specificity: 87.5%) according to the previous report. The ^{99m}Tc-PYP scintigraphy positivity in patients with RapLSI $\geq$ 1.0 and the peak LSR in LA $\leq$ 0.47 s^{-1} was 83.3% (5/6), and the ^{99m}Tc-PYP scintigraphy negativity in patients with RapLSI $<$ 1.0 and the peak LSR in LA $>$ 0.47 s^{-1} was 96.6% (28/29).

Conclusions Left atrial and LV strain analysis were significantly associated with ^{99m}Tc-PYP scintigraphy positivity in ATTR-CM patients with moderate to severe AS. The combination of the peak LSR in LA and RapLSI might be a useful predictor of the presence of ATTR-CM in patients with moderate to severe AS.

Keywords Transthyretin amyloid cardiomyopathy; Aortic stenosis; Two-dimensional speckle tracking echocardiography; Left atrial function; The peak longitudinal strain rate; Relative apical longitudinal strain index

Received: 27 October 2021; Revised: 13 February 2022; Accepted: 7 March 2022
**Correspondence to: Eiichiro Yamamoto, Department of Cardiovascular Medicine, Faculty of Life Sciences, Graduate School of Medical Sciences, Kumamoto University, 1-1-1 Honjo, Chuo-ku, Kumamoto 860-8556, Japan. Tel: +81-96-373-5175; Fax: +81-96-362-3256. Email: eyamamo@kumamoto-u.ac.jp*

© 2022 The Authors. ESC Heart Failure published by John Wiley & Sons Ltd on behalf of European Society of Cardiology.
This is an open access article under the terms of the Creative Commons Attribution-NonCommercial-NoDerivs License, which permits use and distribution in any medium, provided the original work is properly cited, the use is non-commercial and no modifications or adaptations are made.

Introduction

Transthyretin amyloid cardiomyopathy (ATTR-CM) is being increasingly recognized because of ageing of populations, advances in diagnostic abilities, and the potential benefits of emerging therapies.[1] In contrast, aortic stenosis (AS) is one of the most common valvular diseases in elderly patients.[2] The incidence of both ATTR-CM and AS increases with age, and one study showed that 16% of patients with severe AS had concomitant amyloid cardiomyopathy.[3] In addition, patients with amyloid cardiomyopathy appear to have significantly worse outcomes after aortic valve replacement than do patients with isolated AS.[3] Therefore, it is important to diagnose concomitant cardiac amyloidosis in patients with AS to determine the most appropriate treatment plan and to predict the prognosis of these patients.

Two-dimensional (2D) speckle tracking echocardiography is a robust and sensitive echocardiographic technique for quantitative assessment of left atrial (LA) function and has been proven to play an adjunctive role in the diagnosis and prognostic stratification of amyloid cardiomyopathy.[4] However, there was no report about the usefulness of LA function by using 2D speckle tracking echocardiography to diagnose concomitant ATTR-CM in patients with AS.

Although a precise diagnosis of amyloid cardiomyopathy generally requires endomyocardial biopsy, this procedure is invasive. Bone scintigraphy, including ^{99m}Tc-pyrophosphate (PYP) scintigraphy, was recently shown to be remarkably sensitive and specific for the diagnosis of ATTR-CM.[5] Thus, it is considered to be the useful modality to diagnose ATTR-CM.[6]

In this study, we used ^{99m}Tc-PYP scintigraphy to determine concomitant ATTR-CM in patients with AS and evaluated the utility of LA and left ventricular (LV) function using 2D speckle tracking echocardiography for the diagnosis of ATTR-CM in patients with AS.

Methods

Study population

In total, 617 patients underwent ^{99m}Tc-PYP scintigraphy because of suspicion of ATTR-CM at Kumamoto University Hospital from January 2012 to September 2020. Of these 617 patients, there were 75 patients who had moderate to severe AS. Because three patients had insufficient information for evaluation by 2D speckle tracking echocardiography, the remaining 72 patients were finally enrolled in this study (*Figure 1*). ^{99m}Tc-PYP scintigraphy, echocardiography, and laboratory examinations were performed while the patients were in a clinically stable and non-congested condition. We divided these 72 patients into 2 groups based on their ^{99m}Tc-PYP scintigraphy positivity or negativity.

This study conformed to the principles outlined in the Declaration of Helsinki. It was approved by the institutional review board and ethics committee of Kumamoto University (No. 2334). The requirement for informed consent was waived because of the low-risk nature of this retrospective study and the inability to obtain consent directly from all participants. Instead, we extensively announced the study protocol at Kumamoto University Hospital and on our website (http://www.kumadai-junnai.com) and gave patients the opportunity to withdraw from the study.

^{99m}Tc-PYP scintigraphy protocol

^{99m}Tc-PYP scintigraphy was performed using a dual-head single-photon emission computed tomography/CT (Symbia T16; Siemens Healthcare, Erlangen, Germany) with low-energy high-resolution collimators. All patients were scanned 3 h after an intravenous injection of 370–740 MBq of ^{99m}Tc-PYP (Fujifilm RI Pharma, Tokyo, Japan). Anterior

Figure 1 Flow chart of enrolment protocol.

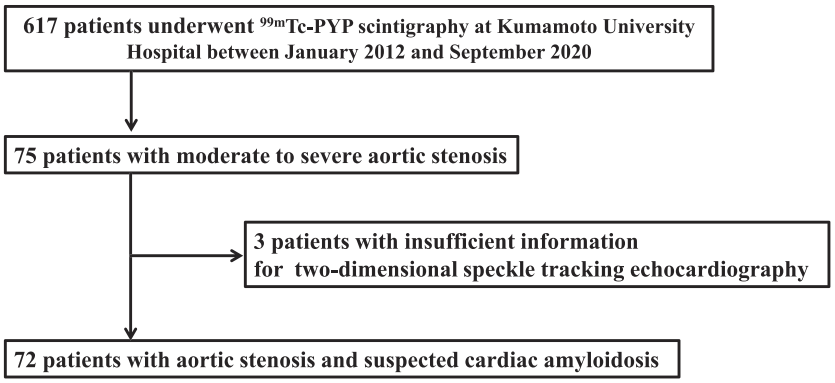

and lateral thoracic planar views were obtained over 3 min duration. The acquisition parameters used for planar imaging were 256 × 256 matrix with 1.23 zoom factor. With the same system, thoracic single-photon emission computed tomography images were acquired for each patient immediately after the planar scan. Cardiac accumulation of ^{99m}Tc-PYP in all patients was assessed by a board-certified nuclear medicine radiologist. On planar images, myocardial tracer uptake was evaluated with a visual scoring method (0 = no myocardial uptake, 1 = myocardial uptake less than rib uptake, 2 = myocardial uptake equal to rib uptake, and 3 = myocardial uptake greater than rib uptake). Myocardial uptake was also analysed quantitatively based on the heart-to-contralateral ratio of the total counts in a region of interest over the heart, which was divided by the background count of a copied and mirrored region of interest over the contralateral chest. ^{99m}Tc-PYP positivity was based on a visual grade 2 or 3 uptake and the heart-to-contralateral ratio of $\geq$1.3.[5,7–9]

Transthoracic echocardiography analysis

Transthoracic echocardiography was performed using commercially available ultrasound equipment. The median duration from echocardiography to ^{99m}Tc-PYP scintigraphy was 26 days (interquartile range, 8–27 days). The chamber size, wall thickness, and left ventricular ejection fraction (LVEF) were evaluated using standard procedures.[10] The peak early and late diastolic velocity of LV inflow (E and A velocity, respectively), the systolic mitral annular velocity (s'), the peak early diastolic velocity (e'), and the late diastolic mitral annular velocity (a') on the septal corner of the mitral annulus were measured in the apical four-chamber view, and the E/e' ratio was calculated. The LV mass index was calculated using a previously described formula.[11] We defined AS in our study as moderate to severe AS. Valvular heart diseases and their severities were defined according to the American Heart Association guideline.[12]

Two-dimensional speckle tracking echocardiography was performed using vendor-independent software (TOMTEC Imaging Systems, Munich, Germany). LV apical views (apical four-chamber, two-chamber, and long-axis views) were acquired at maximum image quality for assessment of the LV LS. Speckles were tracked frame by frame throughout the LV myocardium over the course of one cardiac cycle; basal, mid, and apical regions of interest were then created and manually adjusted whenever needed. The LV endocardial borders were traced at the end-diastolic frame. End-diastole was defined by the QRS complex or as the frame after mitral valve closure. The software then automatically generated LV strain profiles. Segmental LS was automatically demonstrated in a bullseye 16-segment model. Global longitudinal strain (GLS) was calculated as an average peak strain from the three apical projections. The relative apical LS index (RapLSI) was defined using the following equation: [average apical LS/ (average basal LS + average mid LS)].[13]

We also used the above-mentioned 2D speckle tracking software to study LA deformation. The LA LS and LS rate (LSR) was measured using strain indices calculated as the average of the three segments (septal, roof, and lateral) obtained using the apical four-chamber view.[14] LA reservoir function was estimated using the peak LS and the peak LSR during ventricular systole, which represents LA filling during LV systole (*Figure 2A*, *2B*). LA conduit function was estimated using the early LSR during LV diastole (*Figure 2B*). LA pump function was estimated using the late LSR during LV diastole[15–17] (*Figure 2B*). Strain and strain rate are described in absolute values. Echocardiography reviewers were blinded at all times to the patients' clinical history and data to minimize bias.

Analysis of intraobserver and interobserver variability among 20 reassessed patients showed good correlations for peak LSR measurements [average intraclass correlation coefficient, 0.97; 95% confidence interval (CI), 0.93–0.99 and 0.91; 95% CI, 0.79–0.96, respectively].

Statistical analysis

Continuous variables are presented as mean ± standard deviation. High-sensitivity cardiac troponin T and B-type natriuretic peptide (BNP) were not normally distributed, so we selected natural logarithm (Ln) TnT and Ln BNP. Differences in continuous variables were analysed by the unpaired *t*-test or Mann–Whitney *U*-test, as appropriate. Categorical values are presented as number (percentage) and were compared using the χ^2 test. Receiver operating characteristic (ROC) curve analysis was performed to compare the diagnostic accuracy and determine the cut-off values of the peak LSR and RapLSI for ^{99m}Tc-PYP scintigraphy positivity. The independent variables associated with ^{99m}Tc-PYP scintigraphy positivity were assessed by logistic regression analysis. To evaluate the independent variables associated with ^{99m}Tc-PYP scintigraphy positivity, the following variables were initially incorporated into univariate logistic regression analysis models: age, sex, hypertension, diabetes mellitus, dyslipidaemia, smoking, Ln TnT, Ln BNP, LVEF, posterior wall thickness (PWT), LV mass index, E/e', e', s', calcium channel blocker use, angiotensin-converting enzyme inhibitor or angiotensin II receptor blocker use, beta-blocker use, RapLSI, EF/GLS, peak LS, peak LSR, early LSR, and late LSR. Multivariable logistic regression analysis was performed using significant factors in the univariate logistic regression analysis after excluding variables with strong internal correlation and variables which might be important clinically. Pearson's correlation coefficient was used to investigate the correlations between the peak LSR and other LA strain findings. Differences in predictability between parameters were also assessed by calculating the category-free net reclassification improvement (NRI) and the integrated

Figure 2 Representative example of left atrium (LA) measurement by two-dimensional speckle tracking echocardiography. LA strain measures [peak longitudinal strain (LS) = LA reservoir function] (*A*), LA strain rate measures [peak LS rate (LSR) = LA reservoir function, early LSR = LA conduit function, late LSR = LA pump function] (*B*).

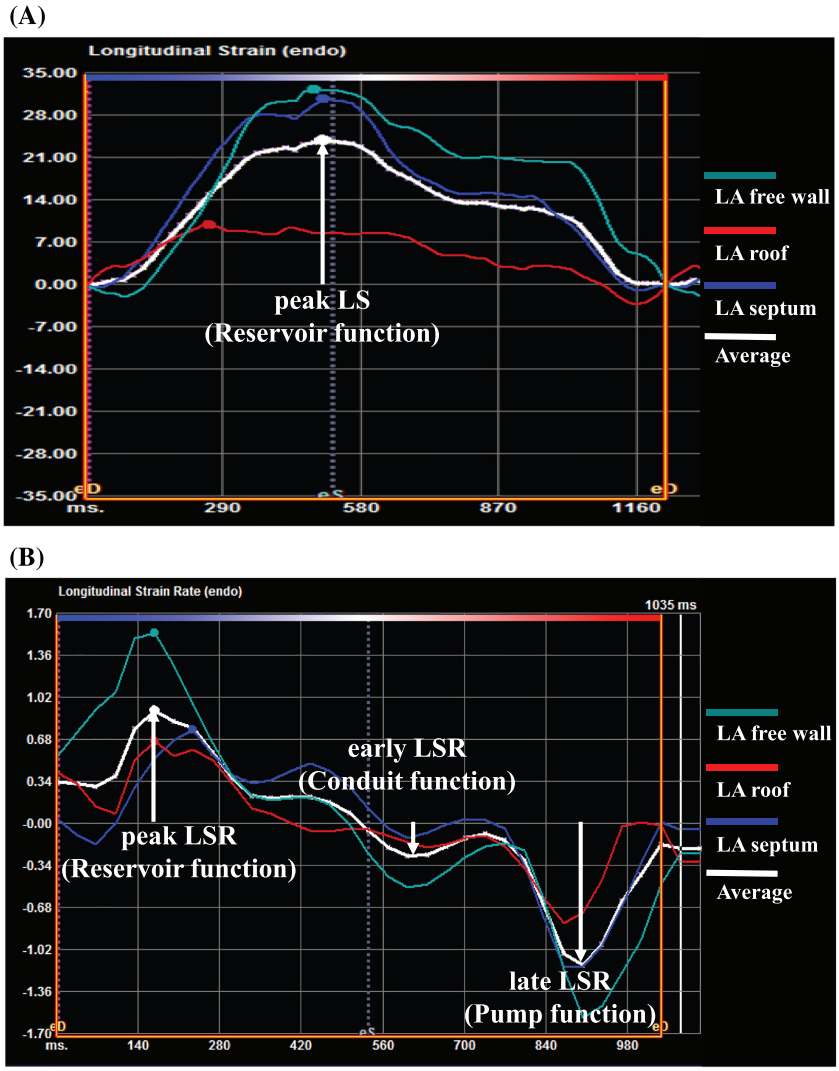

discrimination improvement (IDI) in logistic model. All statistical tests were two-sided. A *P* value of <0.05 was considered statistically significant. Statistical analyses were performed using SPSS Version 24 (IBM Corp., Armonk, NY, USA) and R programme Version 4.0.2 (package 'PredictABEL').[18]

Results

Baseline clinical characteristics, laboratory findings, and medications

Among 72 patients with AS who underwent ^{99m}Tc-PYP scintigraphy, 16 patients (22%) were positive, and 56 patients (78%) were negative for ^{99m}Tc-PYP scintigraphy. In the ^{99m}Tc-PYP scintigraphy-positive group, 12 patients underwent tissue biopsy, of whom 9 (75.0%) had TTR amyloid deposition. Among them, 8 patients underwent endomyocardial biopsy and TTR amyloid deposition in the heart was confirmed in all cases. DNA analysis was performed for 6 patients in the ^{99m}Tc-PYP scintigraphy-positive group and all patients did not have a TTR mutation (ATTRv).

Table 1 summarizes the baseline clinical characteristics, laboratory findings, and medications between the ^{99m}Tc-PYP scintigraphy-positive and scintigraphy-negative groups. There were no significant differences in age, sex, history of cardiovascular risk factors (hypertension, diabetes mellitus, dyslipidaemia, and smoking), Ln BNP, eGFR, or medications [beta-blocker, angiotensin-converting enzyme inhibitor

Table 1 Comparison of baseline clinical characteristics, laboratory findings, and medications between the ^{99m}Tc-PYP scintigraphy-positive and scintigraphy-negative groups

	All (n = 72)	^{99m}Tc-PYP scintigraphy-positive (n = 16)	^{99m}Tc-PYP scintigraphy-negative (n = 56)	P value
Age (years)	82.6 ± 7.7	85.1 ± 3.2	81.8 ± 8.4	0.19
Male sex, n (%)	32 (44.4)	7 (43.8)	25 (44.6)	0.95
NYHA III–IV, n (%)	12 (16.7)	3 (18.8)	9 (16.1)	0.41
Hypertension, n (%)	60 (83.3)	13 (81.3)	47 (83.9)	0.53
DM, n (%)	18 (25.0)	4 (25.0)	14 (25.0)	0.64
Dyslipidaemia, n (%)	40 (55.6)	9 (56.3)	31 (55.4)	0.95
Smoking, n (%)	27 (48.2)	5 (31.3)	22 (39.3)	0.46
Atrial fibrillation, n (%)	11 (15.3)	2 (12.5)	9 (16.1)	0.54
Severe AS, n (%)	51 (70.8)	8 (50.0)	43 (76.8)	<0.05
Ln TnT	−3.3 ± 0.8	−2.9 ± 0.5	−3.5 ± 0.8	<0.05
Ln BNP	5.4 ± 1.0	5.5 ± 0.7	5.3 ± 1.1	0.20
eGFR (mL/min/1.73 m^2)	46.3 ± 20.4	48.1 ± 9.5	45.1 ± 21.8	0.52
Haemoglobin (g/dL)	11.5 ± 1.7	11.8 ± 0.9	11.4 ± 1.9	0.23
Beta-blockers, n (%)	21 (29.2)	5 (31.3)	16 (28.6)	0.53
ACE-I or ARB, n (%)	34 (47.2)	6 (37.5)	28 (50.0)	0.38
CCB, n (%)	38 (52.8)	7 (43.8)	31 (55.4)	0.41
Diuretics, n (%)	32 (44.4)	10 (62.5)	22 (39.3)	0.10

ACE-I, angiotensin-converting enzyme inhibitor; ARB, angiotensin II receptor blocker; AS, aortic stenosis; BNP, B-type natriuretic peptide; CCB, calcium channel blocker; DM, diabetes mellitus; eGFR, estimated glomerular filtration rate; Ln TnT, natural logarithm troponin T; NYHA, New York Heart Association; PYP, pyrophosphate.
Data are presented as mean ± standard deviation and number (percentage). The P values were obtained by unpaired t-test, Mann–Whitney U-test, or χ^2 test.

(ACE-I) or angiotensin II receptor blocker (ARB), calcium channel blocker (CCB) and loop diuretics] between these 2 groups. In contrast, Ln TnT was significantly higher in the ^{99m}Tc-PYP scintigraphy-positive than scintigraphy-negative group (−2.9 ± 0.5 vs. -3.5 ± 0.8, $P < 0.05$).

Conventional transthoracic echocardiography findings

Table 2 summarizes the conventional transthoracic echocardiography findings between the ^{99m}Tc-PYP scintigraphy-positive and scintigraphy-negative groups. A velocity and s' were significantly lower and IVST, PWT, and RWT were significantly higher in the ^{99m}Tc-PYP scintigraphy-positive than scintigraphy-negative group (A velocity: 87 ± 38 cm/s vs. 107 ± 33 cm/s, $P < 0.05$ and s': 3.7 ± 1.0 cm/s vs. 4.7 ± 1.2 cm/s, $P < 0.05$, IVST: 14.6 ± 2.6 mm vs. 13.0 ± 2.5 mm, $P < 0.05$, PWT: 14.6 ± 3.3 mm vs. 12.4 ± 2.1 mm, $P < 0.05$ and RWT: 0.70 ± 0.15 vs. 0.58 ± 0.14, $P < 0.05$, respectively). There were no significant differences in the severity of AS evaluated by transaortic maximum velocity (Vmax) and aortic valve area obtained by Doppler echocardiography between these two groups.

Two-dimensional speckle tracking echocardiography

Table 3 showed the 2D speckle tracking echocardiography between the ^{99m}Tc-PYP scintigraphy-positive and scintigraphy-negative groups. In LV strain analysis, there were no significant differences in GLS, apical LS, and LVEF/GLS ratio between these two groups. In contrast, mid LS and basal LS were significantly lower and RapLSI was significantly higher in the ^{99m}Tc-PYP scintigraphy-positive than scintigraphy-negative group (mid LS: 9.6 ± 2.7% vs. 11.6 ± 3.4%, $P < 0.05$, basal LS: 7.0 ± 3.3% vs. 10.3 ± 3.5%, $P < 0.05$ and RapLSI: 1.09 ± 0.49 vs. 0.78 ± 0.23, $P < 0.05$). In LA strain analysis, the peak LS, the peak LSR, and the late LSR were significantly lower in the ^{99m}Tc-PYP scintigraphy-positive than scintigraphy-negative group (peak LS: 9.6 ± 4.5% vs. 15.2 ± 5.6%, $P < 0.05$, peak LSR: 0.36 ± 0.14 s^{-1} vs. 0.55 ± 0.20 s^{-1}, $P < 0.05$ and late LSR: 0.26 ± 0.25 s^{-1} vs. 0.52 ± 0.29 s^{-1}, $P < 0.05$, respectively). There was no significant difference in the early LSR between these two groups.

Logistic regression analysis for ^{99m}Tc-PYP scintigraphy positivity

As shown in *Table 4*, the univariate logistic regression analysis showed that the Ln TnT, PWT, s', RapLSI, peak LS, peak LSR, and late LSR were associated with ^{99m}Tc-PYP scintigraphy positivity. Because the peak LS and late LSR had strong internal correlation with the peak LSR (peak LS: r = 0.88, $P < 0.05$ and late LSR: r = −0.57; $P < 0.05$, respectively), we incorporated the Ln TnT, PWT, s', RapLSI, peak LSR, age, sex, atrial fibrillation, hypertension, diabetes mellitus, dyslipidaemia, and smoking into the multivariable logistic regression analysis. As a result, multivariable logistic analysis using five forced inclusion models identified that peak LSR and RapLSI were

Table 2 Comparison of conventional TTE findings between the ^{99m}Tc-PYP scintigraphy-positive and scintigraphy-negative groups

	All (n = 72)	^{99m}Tc-PYP scintigraphy-positive (n = 16)	^{99m}Tc-PYP scintigraphy-negative (n = 56)	P value
LVEF (%)	59.4 ± 8.9	57.8 ± 8.2	59.9 ± 9.2	0.22
LVDd (mm)	43.1 ± 6.1	42.1 ± 4.5	43.5 ± 6.5	0.43
IVST (mm)	13.3 ± 2.6	14.6 ± 2.6	13.0 ± 2.5	<0.05
PWT (mm)	12.9 ± 2.5	14.6 ± 3.3	12.4 ± 2.1	<0.05
RWT	0.61 ± 0.15	0.70 ± 0.15	0.58 ± 0.14	<0.05
LVMI (g/m^2)	176 ± 56	197 ± 68	170 ± 51	0.12
LAVI (mL/m^2)	64.4 ± 20.2	65.8 ± 20.2	64.1 ± 20.4	0.66
SV (mL)	67.2 ± 23.9	59.4 ± 20.3	67.8 ± 25.0	0.10
E velocity (cm/s)	81.5 ± 27.1	80.9 ± 25.0	81.6 ± 27.9	0.93
A velocity (cm/s)	103 ± 34	87 ± 38	107 ± 33	<0.05
E/A	0.89 ± 0.74	1.30 ± 1.35	0.77 ± 0.37	0.21
E/e'	21.3 ± 9.1	22.1 ± 8.9	21.1 ± 9.4	0.41
e' (cm/s)	3.9 ± 1.5	3.7 ± 1.2	4.0 ± 1.6	0.72
a' (cm/s)	7.2 ± 2.5	6.3 ± 2.9	7.5 ± 2.4	0.10
s' (cm/s)	4.5 ± 1.2	3.7 ± 1.0	4.7 ± 1.2	<0.05
Vmax (m/s)	4.2 ± 0.7	3.9 ± 0.7	4.3 ± 0.7	0.06
AVA (doppler) (cm^2)	0.71 ± 0.27	0.74 ± 0.25	0.71 ± 0.28	0.48

a', tissue Doppler late diastolic mitral annular velocity; AS, aortic stenosis; ATTR-CM, transthyretin amyloid cardiomyopathy; AVA (doppler), aortic valve area obtained by Doppler echocardiography; A velocity, atrial filling velocity; E/A, ratio of E velocity to A velocity; E/e', the ratio of early transmitral flow velocity to tissue Doppler early diastolic mitral annular velocity; E velocity, early diastolic mitral flow velocity; IVST interventricular septum thickness; LAVI, left atrial volume index; LVDd, left ventricular diastolic diameter; LVEF, left ventricular ejection fraction; LVMI, left ventricular mass index; PWT, posterior wall thickness; PYP, pyrophosphate; RWT, relative wall thickness; s', systolic mitral annular velocity; SV, stroke volume; Vmax, transaortic maximum velocity.
Data are presented as mean ± standard deviation. The P values were obtained by unpaired t-test or Mann–Whitney U-test.

Table 3 Comparison of 2D speckle tracking echocardiography between ^{99m}Tc-PYP scintigraphy-positive and scintigraphy-negative patients

	All (n = 72)	^{99m}Tc-PYP scintigraphy-positive (n = 16)	^{99m}Tc-PYP scintigraphy-negative (n = 56)	P value
GLS (%)	12.8 ± 3.3	11.4 ± 2.5	13.3 ± 3.4	0.43
Apical LS (%)	16.7 ± 5.0	16.4 ± 3.7	16.9 ± 5.4	0.74
Mid LS (%)	11.1 ± 3.3	9.6 ± 2.7	11.6 ± 3.4	<0.05
Basal LS (%)	9.6 ± 3.7	7.0 ± 3.3	10.3 ± 3.5	<0.05
Relative apical LS index	0.85 ± 0.32	1.09 ± 0.49	0.78 ± 0.23	<0.05
LVEF/GLS	4.6 ± 1.6	5.1 ± 1.3	4.5 ± 1.7	0.10
Peak LS (%)	14.0 ± 5.8	9.6 ± 4.5	15.2 ± 5.6	<0.05
Peak LSR (1/s)	0.51 ± 0.20	0.36 ± 0.14	0.55 ± 0.20	<0.05
Early LSR (1/s)	0.38 ± 0.21	0.39 ± 0.22	0.37 ± 0.21	0.77
Late LSR (1/s)	0.47 ± 0.30	0.26 ± 0.25	0.52 ± 0.29	<0.05

AS, aortic stenosis; ATTR-CM, transthyretin amyloid cardiomyopathy; GLS, global longitudinal strain; LS, longitudinal strain; LSR, longitudinal strain rate; LVEF/GLS, ratio of left ventricular ejection fraction to GLS; PYP, pyrophosphate; relative apical LS index, average apical LS/(average basal LS + average mid LS).
Data are presented as mean ± standard deviation. The P values were obtained by unpaired t-test or Mann–Whitney U-test.

independently and significantly associated with ^{99m}Tc-PYP scintigraphy positivity (*Table 5*).

Category-free net reclassification improvement and integrated discrimination improvement in logistic model

The NRI and IDI of the peak LSR for the relative apical LS index were 0.46 (95% CI, −0.08 to 1.00; P = 0.09) and 0.05 (95% CI, −0.12 to 0.21; P = 0.56), respectively. The NRI and IDI of the peak LSR for the s' were 0.59 (95% CI, 0.07–1.11; $P < 0.05$) and 0.08 (95% CI, −0.019 to 0.17; P = 0.12), respectively. Considered by NRI, the peak LSR tended to improve the discrimination ability compared with s'.

Receiver operating characteristic analysis for ^{99m}Tc-PYP scintigraphy positivity

In the ROC analysis of peak LSR for ^{99m}Tc-PYP scintigraphy positivity, the area under the curve (AUC) was 0.79 (95% CI, 0.66–0.91; $P < 0.05$), and the best cut-off value of the peak LSR was 0.47 s^{-1} (sensitivity: 78.6%, specificity: 72.3%) for prediction of ^{99m}Tc-PYP scintigraphy positivity (*Figure 3A*). In the ROC analysis of RapLSI for ^{99m}Tc-PYP scintigraphy positivity, the AUC was 0.69 (95% CI, 0.54–0.84; $P < 0.05$).

Table 4 Univariate logistic regression analysis for ^{99m}Tc-PYP scintigraphy positivity

	Univariate analysis		
Variables	Odds ratio	95% CI	*P* value
Age	1.09	0.98–1.21	0.13
Sex (male)	0.96	0.31–2.95	0.94
Hypertension	0.83	0.20–3.52	0.80
DM	1.00	0.28–3.61	1.00
Dyslipidaemia	1.04	0.34–3.18	0.95
Smoking	0.64	0.20–2.11	0.46
Atrial fibrillation	1.33	0.36–4.94	0.67
Ln TnT	2.86	1.23–6.67	<0.05
Ln BNP	1.47	0.82–2.65	0.20
LVEF	0.98	0.92–1.04	0.40
PWT(*100)	1.04	1.01–1.06	<0.05
LVMI	1.00	1.00–1.00	0.65
E/e'	1.01	0.95–1.07	0.71
e'	0.90	0.59–1.37	0.62
s'	0.45	0.25–0.81	<0.05
CCB	0.63	0.21–1.92	0.41
ACE-I or ARB	0.60	0.19–1.88	0.38
Beta-blockers	1.14	0.34–3.79	0.84
RapLSI (*100)	1.03	1.01–1.05	<0.05
EF/GLS	1.26	0.89–1.78	0.21
Peak LS	0.79	0.69–0.92	<0.05
Peak LSR (*100)	0.93	0.89–0.97	<0.05
Early LSR (*100)	1.00	0.97–1.03	0.98
Late LSR (*100)	1.04	1.01–1.06	<0.05

ACE-I, angiotensin-converting enzyme inhibitor; ARB, angiotensin II receptor blocker; AS, aortic stenosis; ATTR-CM, transthyretin amyloid cardiomyopathy; BNP, B-type natriuretic peptide; CCB, calcium channel blocker; CI, confidence interval; DM, diabetes mellitus; E/e', the ratio of early transmitral flow velocity to tissue Doppler early diastolic mitral annular velocity; EF/GLS, the ratio of left ventricular ejection fraction to global longitudinal strain; Ln TnT, natural logarithm troponin T; LS, longitudinal strain; LSR, longitudinal strain rate; LVEF, left ventricular ejection fraction; LVMI, left ventricular mass index; PWT, posterior wall thickness; PYP, pyrophosphate; relative apical LS index, average apical longitudinal strain (LS)/(average basal LS + average mid LS); s', systolic mitral annular velocity.

Table 5 Multivariable logistic regression analysis for ^{99m}Tc-PYP scintigraphy positivity

	Multivariable analysis		
Models	Odds ratio	95% CI	*P* value
Model 1			
Peak LSR (*100)	0.94	0.89–0.98	<0.05
RapLSI (*100)	1.03	1.00–1.06	<0.05
s'	0.72	0.37–1.42	0.35
Model 2			
Peak LSR (*100)	0.93	0.89–0.98	<0.05
RapLSI (*100)	1.03	1.00–1.06	<0.05
PWT (*100 cm)	1.03	0.99–1.06	0.09
Model 3			
Peak LSR (*100)	0.93	0.89–0.98	<0.05
RapLSI (*100)	1.03	1.00–1.07	<0.05
Ln TnT	1.91	0.69–5.36	0.21
Model 4			
Peak LSR (*100)	0.92	0.86–0.98	<0.05
RapLSI (*100)	1.03	1.00–1.07	<0.05
Age	1.16	0.97–1.39	0.11
Sex	1.50	0.35–6.42	0.58
Atrial fibrillation	0.49	0.07–3.46	0.48
Model 5			
Peak LSR (*100)	0.89	0.83–0.96	<0.05
RapLSI (*100)	1.04	1.01–1.08	<0.05
Hypertension	0.15	0.01–1.82	0.14
Diabetes mellitus	2.77	0.41–18.6	0.30
Dyslipidaemia	0.60	0.13–2.77	0.51
Smoking	1.63	0.33–8.14	0.55

CI, confidence interval; Ln TnT, natural logarithm troponin T; LSR, longitudinal strain rate; PWT, posterior wall thickness; PYP, pyrophosphate; RapLSI; relative apical LS index; s', systolic mitral annular velocity.

Because it was difficult to decide the cut-off point by ROC analysis, we decided the cut-off point of RapLSI as 1.00 according to the previous report[13] (*Figure 3B*).

Predictive model for ^{99m}Tc-PYP scintigraphy positivity

Using peak LSR $\leq$ 0.47 s^{-1}, we examined ^{99m} Tc-PYP scintigraphy positivity. The ^{99m}Tc-PYP scintigraphy positivity in patients with the peak LSR in LA $\leq$ 0.47 s^{-1} was 39.4% (13/33), and the ^{99m}Tc-PYP scintigraphy negativity in patients with the peak LSR in LA $>$ 0.47 s^{-1} was 92.3% (36/39).

In addition to peak LSR, using RapLSI $\geq$ 1.0, we examined ^{99m} Tc-PYP scintigraphy positivity. We divided the study patients into three groups according to the number of positive for each factor: 2-point group (peak LSR $\leq$ 0.47 s^{-1} and RapLSI $\geq$ 1.0, n = 6), 1-point group (peak LSR $\leq$ 0.47 s^{-1} and RapLSI $<$ 1.0, or peak LSR $>$ 0.47 s^{-1} and RapLSI $\geq$ 1.0, n = 37), and 0-point group (peak LSR $>$ 0.47 s^{-1} and RapLSI $<$ 1.0, n = 29). About 83.3% of 2-point group had a positive ^{99m}Tc-PYP scintigraphy. In contrast, 96.6% of 0-point group had a negative ^{99m}Tc-PYP scintigraphy (*Figure 4*).

Subgroup analysis

Next, we divided patients into severe and moderate AS group according to peak aortic valve velocity (severe AS: Vmax $\geq$ 4.0 m/s, moderate AS: Vmax $<$ 4.0 m/s).

In severe AS group, the univariate logistic regression analysis showed that the peak LSR and RapLSI were significantly associated with ^{99m}Tc-PYP scintigraphy positivity (Supporting Information, *Table S1a*). In the ROC analysis, the AUC of peak LSR and RapLSI for ^{99m}Tc-PYP scintigraphy positivity were 0.75 (95% CI, 0.58–0.92; P $<$ 0.05) (*Figure S1a*) and 0.69 (95% CI, 0.47–0.90; P = 0.09) (*Figure S1b*), respectively.

In moderate AS group, the univariate logistic regression analysis also showed that the peak LS and peak LSR were significantly associated with ^{99m}Tc-PYP scintigraphy positivity (*Table S1b*). In the ROC analysis, the AUC of peak LSR and RapLSI for ^{99m}Tc-PYP scintigraphy positivity were 0.80 (95% CI, 0.60–1.00; P $<$ 0.05) (*Figure S2a*) and 0.66 (95% CI, 0.42–0.91; P = 0.22) (*Figure S2b*), respectively.

Figure 3 Receiver operating characteristic analysis for ^{99m}Tc-pyrophosphate (PYP) scintigraphy positivity in patients with aortic stenosis suspected to have transthyretin amyloid cardiomyopathy. Area under the curve (AUC) of peak longitudinal strain rate (LSR) was 0.79 (95% confidence interval (CI), 0.66–0.91; $P < 0.05$) (*A*). AUC of relative apical longitudinal strain index (RapLSI) was 0.69 (95% CI, 0.54–0.84; $P < 0.05$) (*B*).

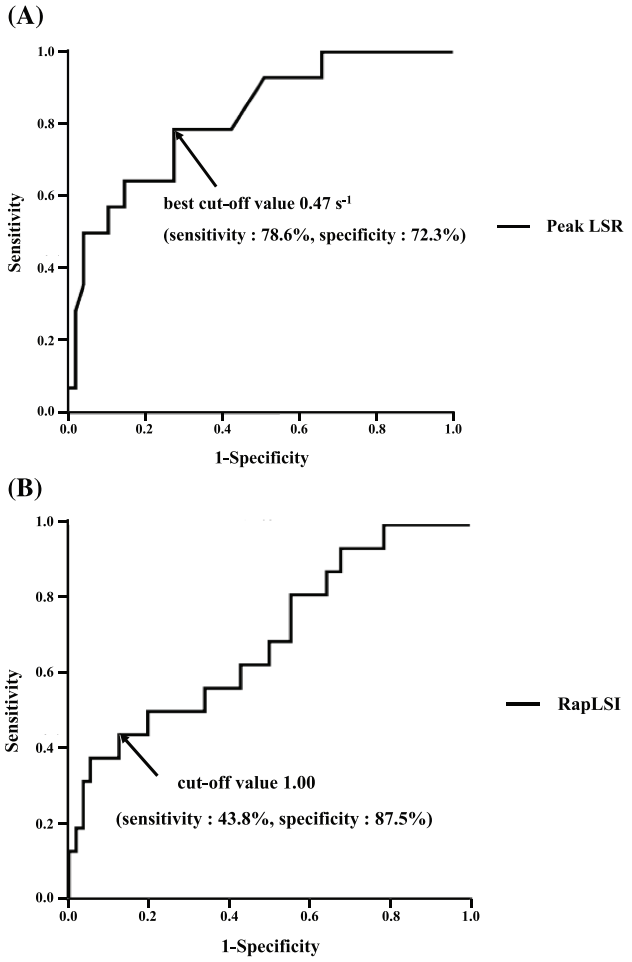

Figure 4 Predictive model for ^{99m}Tc-pyrophosphate (PYP) scintigraphy. We divided the study patients into three groups according to the number of positive for each factor: 2-point group (peak longitudinal strain rate (LSR) $\leq$ 0.47 s^{-1} and relative apical longitudinal strain index (RapLSI) $\geq$ 1.0, n = 6), 1-point group (peak LSR $\leq$ 0.47 s^{-1} and RapLSI $<$ 1.0, or peak LSR $>$ 0.47 s^{-1} and RapLSI $\geq$ 1.0, n = 37), and 0-point group (peak LSR $<$ 0.47 s^{-1} and RapLSI $<$ 1.0, n = 29).

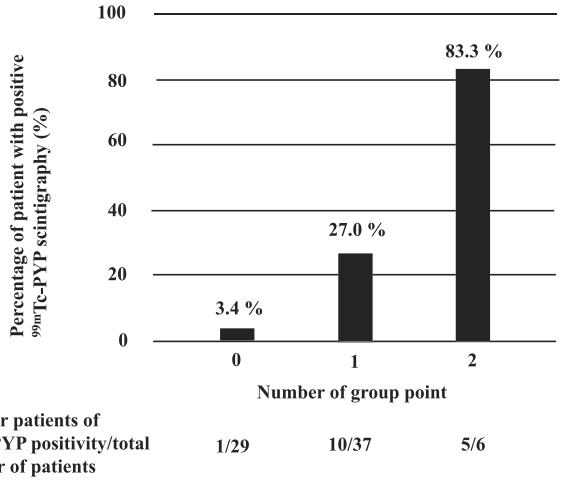

Discussion

The major finding of the present study is that the combination of LA and LV function evaluated by 2D speckle tracking echocardiography was useful to evaluate ATTR-CM in patients with AS.

In these days, non-biopsy diagnosis of ATTR-CM by using bone scintigraphy including ^{99m}Tc-PYP scintigraphy has been established.[4] In our present study, 100% (8/8) of patients with ^{99m}Tc-PYP scintigraphy positivity had amyloid deposition in their hearts, indicating that ^{99m}Tc-PYP scintigraphy was useful to diagnose ATTR-CM even in patients with AS. However, this modality is costly and only available in specialist centres. Therefore, it is important to raise the pretest probability of ^{99m}Tc-PYP scintigraphy positivity by using inexpensive and less invasive methods. LV apical sparing, which is represented as a RapLSI in the present study, is a pattern of regional differences in deformation in which the LS in the basal and middle segments of the left ventricle is more severely impaired than that in the apical segments.[13] LV apical sparing is highly specific for amyloid cardiomyopathy and has incremental diagnostic value over other echocardiographic parameters traditionally used for this purpose.[19] Even in our present study, RapLSI was associated with ^{99m}Tc-PYP scintigraphy positivity. However, the AUC of RapLSI for predicting ^{99m}Tc-PYP scintigraphy positivity were relatively low, indicating that only RapLSI might not be enough to evaluate ATTR-CM in patients with AS. The stress and afterload imposed on the ventricle by a severely calcified and stenotic aortic valve might mask the LV apical sparing that is otherwise detected in a patient with ATTR-CM without AS. These might be the reason why RapLSI had low sensitivity to evaluate ^{99m}Tc-PYP scintigraphy positivity in ATTR-CM patients with AS. Thus, only RapLSI was not enough to evaluate ATTR-CM in patients with AS.

In contrast, our study revealed that LA dysfunction estimated by 2D speckle tracking echocardiography was important diagnostic marker for ATTR-CM in patients with AS. In usual, worse LA function is correlated with a greater impairment of LV systolic and diastolic function.[20] LV systolic and diastolic dysfunction may contribute to LA dysfunction because the influence of downward motion of the mitral plane during ventricular systole leads to reduced systolic expansion of the LA.[4,17,21] In addition, amyloid deposition occurs not only in the LV but also in the LA.[22] Thus, LA dysfunction in patients

with amyloid cardiomyopathy depend on the combination of restrictive LV function with high filling pressures and intrinsic LA function failure by direct amyloid infiltration. In patients without ATTR-CM, LA dysfunction depends on mainly restrictive LV function except for atrial fibrillation. Therefore, LA function is thought to be impaired more in AS patient with ATTR-CM than in those without ATTR-CM in our present study, which might be the reason why LA dysfunction was important diagnostic marker for ATTR-CM in our present study. Although atrial fibrillation is another important factor for LA dysfunction in ATTR-CM patients, atrial fibrillation was not significantly associated with ^{99m}Tc-PYP scintigraphy positivity in our present study. The frequency of atrial fibrillation increases according to the progression of ATTR-CM.[23] In our present study, LVEF of ^{99m}Tc-PYP scintigraphy-positive group was relatively preserved compared with the previous report,[24] suggesting that many ATTR-CM patients in ^{99m}Tc-PYP scintigraphy positive in this study might be diagnosed in the early phase of the disease. These might be the reason why there were only two atrial fibrillation patients in ^{99m}Tc-PYP scintigraphy-positive group and atrial fibrillation was not significantly associated with ^{99m}Tc-PYP scintigraphy positivity in our present study.

Two-dimensional speckle tracking echocardiography is a very helpful technique for investigation of advanced atrial functional components such as the reservoir phase, conduit phase, and active phase, which are otherwise difficult to investigate non-invasively.[25–27] Several studies showed that LA reservoir and active function were impaired in various types of amyloid cardiomyopathy.[4,28] In our present study, the peak LSR, which represents LA reservoir function, was the strongest predictor of ^{99m}Tc-PYP scintigraphy positivity in patients with AS. In addition, late LSR, which represents LA contracting function, was also associated with ^{99m}Tc-PYP scintigraphy positivity. These indicated that both reservoir and active functions were impaired in AS patients with ATTR-CM. In contrast, LA conduit function was not significantly associated with ^{99m}Tc-PYP scintigraphy positivity. Nochioka *et al*. previously reported that LA conduit function did not differ significantly between patients with amyloid cardiomyopathy and control patients.[4] Therefore, LA conduit function is thought to be compensatory mechanism when LA reservoir and contraction function are impaired.

Castaño *et al*.[24] revealed that the s' is an excellent predictor for the concomitant amyloid cardiomyopathy in patients with AS. In our study, however, s' was not significantly associated with ATTR-CM after adjusting for peak LSR and RapLSI. Although Castaño *et al*. evaluated A velocity and LAVI in their study, they did not evaluate LA function in detail.[24] Because s' is related to the absolute value of GLS, s' depends on only LV function.[29] In contrast, peak LSR is affected by both LA and LV function, which might be the reason why peak LSR is more important than s' for diagnosis of ATTR-CM in our present study.

The aim of our study was to raise the pretest probability for ^{99m}Tc-PYP scintigraphy in AS patients by using 2D speckle tracking echocardiography. In our present study, we selected peak LSR and RapLSI as strongly significant factors for ^{99m}Tc-PYP scintigraphy positivity in AS patients. Of note, patients with high peak LSR and low RapLSI were rarely ^{99m}Tc-PYP scintigraphy positive, and almost all of patients with low peak LSR and high RapLSI were ^{99m}Tc-PYP scintigraphy positive. Based on these findings, we recommend performing ^{99m}Tc-PYP scintigraphy for AS patients with low peak LSR and high RapLSI on patients' selection for ^{99m}Tc-PYP scintigraphy. Because concomitant ATTR-CM is associated with a poor prognosis of AS patients,[30] it is important to raise the pretest probability of ^{99m}Tc-PYP scintigraphy positivity by using combination of LA and LV strain analysis estimated by 2D speckle tracking echocardiography for patients with AS.

Study limitations

This study had several limitations. First, it included a small number of patients and was performed at a single centre. Although a similar cohort would be useful to support our results, this is not possible because there are no similar cohorts. Second, we obtained echocardiographic images using several ultrasound vendors. The 2D speckle tracking echocardiography analysis was performed with TomTec Image-Arena™ (vendor-independent) software. Although there are significant correlations in the LS values analysed using vendor-independent software for paired images obtained from different ultrasound vendors,[31] inter-vendor variability still might have affected our study results. Third, there is a possibility of referral bias, although we used a standardized protocol and the ^{99m}Tc-PYP scintigraphy images were interpreted by the same independent operators. Forth, we divided patients into three subgroups to make predictive model for ^{99m}Tc-PYP scintigraphy positivity. However, there were small samples in each subgroup, affecting the possibility to get reliable results statistically. This point was another important limitation in our present study. Despite these limitations, this is the first cohort study to evaluate the usefulness of the combination of LA and LV function evaluated by 2D speckle tracking echocardiography in elderly patients with moderate to severe AS who underwent ^{99m}Tc-PYP scintigraphy for suspected amyloid cardiomyopathy. Further prospective studies involving more patients with AS are needed to validate our results.

Conclusions

Left atrial and LV strain analysis were significantly associated with ^{99m}Tc-PYP scintigraphy positivity in ATTR-CM patients

with moderate to severe AS. Combination of LA and LV strain analysis might be useful to diagnose ATTR-CM in patients with moderate to severe AS.

Acknowledgements

We thank Angela Morben, DVM, ELS, from Edanz Group (https://en-author-services.edanzgroup.com/ac), for editing a draft of this manuscript.

Conflict of interest

The authors report no relationships that could be construed as a conflict of interest.

Funding

This work was supported by a Grant-in-Aid for Scientific Research from the Japan Society for the Promotion of Science (grant 20K08476 to H.U.).

Supporting information

Additional supporting information may be found online in the Supporting Information section at the end of the article.

Figure S1. Receiver operating characteristic analysis for ^{99m}Tc-pyrophosphate (PYP) scintigraphy positivity in patients with severe aortic stenosis suspected to have transthyretin amyloid cardiomyopathy. Area under the curve (AUC) of peak longitudinal strain rate (LSR) was 0.75 (95% confidence interval (CI), 0.58–0.92; $p < 0.05$)(a). AUC of relative apical longitudinal strain index (RapLSI) was 0.69 (95% CI, 0.47–0.90; $p = 0.09$)(b).

Figure S2. Receiver operating characteristic analysis for ^{99m}Tc-pyrophosphate (PYP) scintigraphy positivity in patients with moderate aortic stenosis suspected to have transthyretin amyloid cardiomyopathy. AUC of peak longitudinal strain rate (LSR) was 0.80 (95% CI, 0.60–1.00; $p < 0.05$)(a). AUC of relative apical longitudinal strain index (RapLSI) was 0.66 (95% CI, 0.42–0.91; $p = 0.22$)(b).

Table S1a. Univariate logistic regression analysis for ^{99m}Tc-PYP scintigraphy positivity

Table S1b. Univariate logistic regression analysis for ^{99m}Tc-PYP scintigraphy positivity

References

1. Iung B, Baron G, Butchart EG, Delahaye F, Gohlke-Barwolf C, Levang OW, Tornos P, Vanoverschelde JL, Vermeer F, Boersma E, Ravaud P, Vahanian A. A prospective survey of patients with valvular heart disease in Europe: the euro heart survey on valvular heart disease. *Eur Heart J* 2003; **24**: 1231–1243.
2. Cavalcante JL, Rijal S, Abdelkarim I, Althouse AD, Sharbaugh MS, Fridman Y, Soman P, Forman DE, Schindler JT, Gleason TG, Lee JS, Schelbert EB. Cardiac amyloidosis is prevalent in older patients with aortic stenosis and carries worse prognosis. *J Cardiovasc Magn Reson* 2017; **19**: 98.
3. Nochioka K, Quarta CC, Claggett B, Roca GQ, Rapezzi C, Falk RH, Solomon SD. Left atrial structure and function in cardiac amyloidosis. *Eur Heart J Cardiovasc Imaging* 2017; **18**: 1128–1137.
4. Gillmore JD, Maurer MS, Falk RH, Merlini G, Damy T, Dispenzieri A, Wechalekar AD, Berk JL, Quarta CC, Grogan M, Lachmann HJ, Bokhari S, Castano A, Dorbala S, Johnson GB, Glaudemans AW, Rezk T, Fontana M, Palladini G, Milani P, Guidalotti PL, Flatman K, Lane T, Vonberg FW, Whelan CJ, Moon JC, Ruberg FL, Miller EJ, Hutt DF, Hazenberg BP, Rapezzi C, Hawkins PN. Nonbiopsy diagnosis of cardiac transthyretin amyloidosis. *Circulation* 2016; **133**: 2404–2412.
5. Tahara N, Lairez O, Endo J, Okada A, Ueda M, Ishii T, Kitano Y, Lee HE, Russo E, Kubo T. 99mTechnetium-pyrophosphate scintigraphy: a practical guide for early diagnosis of transthyretin amyloid cardiomyopathy. *ESC Heart Failure* 2022; **9**: 251–262.
6. Castano A, Haq M, Narotsky DL, Goldsmith J, Weinberg RL, Morgenstern R, Pozniakoff T, Ruberg FL, Miller EJ, Berk JL, Dispenzieri A, Grogan M, Johnson G, Bokhari S, Maurer MS. Multicenter study of planar technetium 99m pyrophosphate cardiac imaging: predicting survival for patients with ATTR cardiac amyloidosis. *JAMA Cardiol* 2016; **1**: 880–889.
7. Dorbala S, Ando Y, Bokhari S, Dispenzieri A, Falk RH, Ferrari VA, Fontana M, Gheysens O, Gillmore JD, Glaudemans A, Hanna MA, Hazenberg BPC, Kristen AV, Kwong RY, Maurer MS, Merlini G, Miller EJ, Moon JC, Murthy VL, Quarta CC, Rapezzi C, Ruberg FL, Shah SJ, Slart R, Verberne HJ, Bourque JM. ASNC/AHA/ASE/EANM/HFSA/ISA/SCMR/SNMMI expert consensus recommendations for multimodality imaging in cardiac amyloidosis: part 1 of 2—evidence base and standardized methods of imaging. *J Card Fail* 2019; **25**: e1–e39.
8. Liu D, Hu K, Niemann M, Herrmann S, Cikes M, Störk S, Gaudron PD, Knop S, Ertl G, Bijnens B, Weidemann F. Effect of combined systolic and diastolic functional parameter assessment for differentiation of cardiac amyloidosis from other causes of concentric left ventricular hypertrophy. *Circ Cardiovasc Imaging* 2013; **6**: 1066–1072.
9. Lang RM, Badano LP, Mor-Avi V, Afilalo J, Armstrong A, Ernande L, Flachskampf FA, Foster E, Goldstein SA, Kuznetsova T, Lancellotti P, Muraru D, Picard MH, Rietzschel ER, Rudski L, Spencer KT, Tsang W, Voigt JU. Recommendations for cardiac chamber quantification by echocardiography in adults: an update from the American Society of Echocardiography and the European Association of Cardiovascular Imaging. *J Am Soc Echocardiogr* 2015; **28**: 1–39.e14.
10. Devereux RB, Alonso DR, Lutas EM, Gottlieb GJ, Campo E, Sachs I, Reichek N. Echocardiographic assessment of left ventricular hypertrophy: comparison to necropsy findings. *Am J Cardiol* 1986; **57**: 450–458.

11. Nishimura RA, Otto CM, Bonow RO, Carabello BA, Erwin JP 3rd, Guyton RA, O'Gara PT, Ruiz CE, Skubas NJ, Sorajja P, Sundt TM 3rd, Thomas JD. 2014 AHA/ACC guideline for the management of patients with valvular heart disease: a report of the American College of Cardiology/American Heart Association task force on practice guidelines. *J Am Coll Cardiol* 2014; **63**: e57–e185.
12. Phelan D, Collier P, Thavendiranathan P, Popovic ZB, Hanna M, Plana JC, Marwick TH, Thomas JD. Relative apical sparing of longitudinal strain using two-dimensional speckle-tracking echocardiography is both sensitive and specific for the diagnosis of cardiac amyloidosis. *Heart* 2012; **98**: 1442–1448.
13. Kitaoka H, Izumi C, Izumiya Y, Inomata T, Ueda M, Kubo T, Koyama J, Sano M, Sekijima Y, Tahara N, Tsukada N, Tsujita K, Tsutsui H, Tomita T, Amano M, Endo J, Okada A, Oda S, Takashio S, Baba Y, Misumi Y, Yazaki M, Anzai T, Ando Y, Isobe M, Kimura T, Fukuda K. JCS 2020 guideline on diagnosis and treatment of cardiac amyloidosis. *Circ J* 2020; **84**: 1610–1671.
14. Badano LP, Kolias TJ, Muraru D, Abraham TP, Aurigemma G, Edvardsen T, D'Hooge J, Donal E, Fraser AG, Marwick T, Mertens L, Popescu BA, Sengupta PP, Lancellotti P, Thomas JD, Voigt JU. Standardization of left atrial, right ventricular, and right atrial deformation imaging using two-dimensional speckle tracking echocardiography: a consensus document of the EACVI/ASE/industry task force to standardize deformation imaging. *Eur Heart J Cardiovasc Imaging* 2018; **19**: 591–600.
15. Rossi A, Gheorghiade M, Triposkiadis F, Solomon SD, Pieske B, Butler J. Left atrium in heart failure with preserved ejection fraction: structure, function, and significance. *Circ Heart Fail* 2014; **7**: 1042–1049.
16. Cameli M, Lisi M, Mondillo S, Padeletti M, Ballo P, Tsioulpas C, Bernazzali S, Maccherini M. Left atrial longitudinal strain by speckle tracking echocardiography correlates well with left ventricular filling pressures in patients with heart failure. *Cardiovasc Ultrasound* 2010; **8**: 14.
17. Santos AB, Kraigher-Krainer E, Gupta DK, Claggett B, Zile MR, Pieske B, Voors AA, Lefkowitz M, Bransford T, Shi V, Packer M, McMurray JJ, Shah AM, Solomon SD. Impaired left atrial function in heart failure with preserved ejection fraction. *Eur J Heart Fail* 2014; **16**: 1096–1103.
18. Kundu S, Aulchenko YS, Cecile A & Janssens JW 2020. PredictABEL: assessment of risk prediction models. R package version 1.2-4. https://CRAN.R-project.org/package=PredictABEL. Accessed 15 March 2021.
19. Quarta CC, Solomon SD, Uraizee I, Kruger J, Longhi S, Ferlito M, Gagliardi C, Milandri A, Rapezzi C, Falk RH. Left ventricular structure and function in transthyretin-related versus light-chain cardiac amyloidosis. *Circulation* 2014; **129**: 1840–1849.
20. Santos AB, Roca GQ, Claggett B, Sweitzer NK, Shah SJ, Anand IS, Fang JC, Zile MR, Pitt B, Solomon SD, Shah AM. Prognostic relevance of left atrial dysfunction in heart failure with preserved ejection fraction. *Circ Heart Fail* 2016; **9**: e002763.
21. Barbier P, Solomon SB, Schiller NB, Glantz SA. Left atrial relaxation and left ventricular systolic function determine left atrial reservoir function. *Circulation* 1999; **100**: 427–436.
22. Falk RH. Diagnosis and management of the cardiac amyloidoses. *Circulation* 2005; **112**: 2047–2060.
23. Longhi S, Quarta CC, Milandri A, Lorenzini M, Gagliardi C, Manuzzi L, Bacchi-Reggiani ML, Leone O, Ferlini A, Russo A, Gallelli I, Rapezzi C. Atrial fibrillation in amyloidotic cardiomyopathy: prevalence, incidence, risk factors and prognostic role. *Amyloid* 2015; **22**: 147–155.
24. Castaño A, Narotsky DL, Hamid N, Khalique OK, Morgenstern R, DeLuca A, Rubin J, Chiuzan C, Nazif T, Vahl T, George I, Kodali S, Leon MB, Hahn R, Bokhari S, Maurer MS. Unveiling transthyretin cardiac amyloidosis and its predictors among elderly patients with severe aortic stenosis undergoing transcatheter aortic valve replacement. *Eur Heart J* 2017; **38**: 2879–2887.
25. Cameli M, Caputo M, Mondillo S, Ballo P, Palmerini E, Lisi M, Marino E, Galderisi M. Feasibility and reference values of left atrial longitudinal strain imaging by two-dimensional speckle tracking. *Cardiovasc Ultrasound* 2009; **7**: 6.
26. Blume GG, McLeod CJ, Barnes ME, Seward JB, Pellikka PA, Bastiansen PM, Tsang TS. Left atrial function: physiology, assessment, and clinical implications. *Eur J Echocardiogr* 2011; **12**: 421–430.
27. Di Bella G, Minutoli F, Madaffari A, Mazzeo A, Russo M, Donato R, Zito C, Aquaro GD, Piccione MC, Pedri S, Vita G, Pingitore A, Carerj S. Left atrial function in cardiac amyloidosis. *J Cardiovasc Med (Hagerstown)* 2016; **17**: 113–121.
28. de Gregorio C, Dattilo G, Casale M, Terrizzi A, Donato R, Di Bella G. Left atrial morphology, size and function in patients with transthyretin cardiac amyloidosis and primary hypertrophic cardiomyopathy—comparative strain imaging study. *Circ J* 2016; **80**: 1830–1837.
29. Peverill RE, Cheng K, Cameron J, Donelan L, Mottram PM. Relationships of global longitudinal strain with s`, long-axis systolic excursion, left ventricular length and heart rate. *PLoS ONE* 2020; **15**: e0235791.
30. Treibel TA, Fontana M, Gilbertson JA, Castelletti S, White SK, Scully PR, Roberts N, Hutt DF, Rowczenio DM, Whelan CJ, Ashworth MA, Gillmore JD, Hawkins PN, Moon JC. Occult transthyretin cardiac amyloid in severe calcific aortic stenosis: prevalence and prognosis in patients undergoing surgical aortic valve replacement. *Circ Cardiovasc Imaging* 2016; **9**.
31. Nagata Y, Takeuchi M, Mizukoshi K, Wu VC, Lin FC, Negishi K, Nakatani S, Otsuji Y. Intervendor variability of two-dimensional strain using vendor-specific and vendor-independent software. *J Am Soc Echocardiogr* 2015; **28**: 630–641.